the one-residue insertion between the H2 and H3 helices (Fig. 5A). In the threading analysis of ElonginA, the VHL α domain structure ranked 704th, suggesting that the ElonginC-binding domain of ElonginA would be divergent. ElonginA sequences encompassing both the region of homology with the VHL H1 helix and the proposed F-box sequences (residues 545 to 610) were threaded as above.
34. To test for cross-reactivity between the ElonginC and Skp1 components, we coexpressed ElonginB, Skp1, and GST-VHL, isolated the GST-VHL with glutathione beads, and found no Skp1 copurifying with GST-VHL; this suggested that VHL has no affinity for Skp1. Conversely, we coexpressed ElonginB, ElonginC, and GST-Skp2 and found that a small amount of the ElonginC-ElonginB complex associated with GST-Skp2. Upon further purification, this complex did not persist like the VCB complex would, indicating that any ElonginC-Skp2 interaction would be very weak relative to the ElonginC-VHL or the Skp1-Skp2 interaction (C. E. Stebbins, W. G. Kaelin Jr., N. P. Pavletich, data not shown).
35. E. E. Patton, A. R. Willems, M. Tyers, *Trends Genet.* **14**, 236 (1998); E. E. Patton *et al.*, *Genes Dev.* **12**, 692 (1998).
36. Z. Otwinowski and W. Minor, *Methods Enzymol.* **276**, 307 (1997).
37. CCP4, *Acta Crystalogr. D* **50**, 760 (1994).
38. T. A. Jones, J.-Y. Zou, S. W. Cowan, M. Kjeldgaard, *Acta Crystallogr. A* **47**, 110 (1991).
39. A. T. Brünger *et al.*, *Acta Crystallogr. D* **54**, 905 (1998).
40. Single-letter abbreviations for the amino acid residues are as follows: A, Ala; C, Cys; D, Asp; E, Glu; F, Phe; G, Gly; H, His; I, Ile; K, Lys; L, Leu; M, Met; N, Asn; P, Pro; Q, Gln; R, Arg; S, Ser; T, Thr; V, Val; W, Trp; and Y, Tyr.
41. B. Rost and C. Sander, *J. Mol. Biol.* **232**, 584 (1993).
42. Supported by the National Institutes of Health, the Howard Hughes Medical Institute, the Dewitt Wallace Foundation, the Samuel and May Rudin Foundation, and a Frank Lappin Horsfall Jr. Fellowship to C.E.S. We thank S. Geromanos and H. Erdjument-Bromage of the Sloan-Kettering Microchemistry Facility for NH_2-terminal sequence and mass spectroscopic analyses, A. Batchelor for the pBB75 plasmid, M. Sullivan of the National Synchrotron Light Source X9 beam line and the staff of the Cornell High Energy Synchrotron Source MacChess for help with data collection, and C. Murray for administrative help. Coordinates have been deposited with the Brookhaven Protein Data Bank (accession code 1vcb).

1 February 1999; accepted 18 March 1999

Viscosity Near Earth's Solid Inner Core

D. E. Smylie

Anomalous splitting of the two equatorial translational modes of oscillation of Earth's solid inner core is used to estimate the effective viscosity just outside its boundary. Superconducting gravimeter observations give periods of 3.5822 ± 0.0012 (retrograde) and 4.0150 ± 0.0010 (prograde) hours. With the use of Ekman layer theory to estimate viscous drag forces, an inferred single viscosity of 1.22×10^{11} Pascal seconds gives calculated periods of 3.5839 and 4.0167 hours for the two modes, close to the observed values. The large effective viscosity is consistent with a fluid, solid-liquid mixture surrounding the inner core associated with the "compositional convection" that drives Earth's geodynamo.

Earth's solid inner core of 1220-km radius is thought to have formed by freezing of the molten metallic alloy constituting the outer core (*1*). The fluid outer core extending to a radius of 3485 km is about 7% less dense than pure Fe (*2*), and a variety of lighter compounds have been proposed to account for the deficit in density from the Fe-Ni bulk composition implied by Fe meteorites, averaging 8% Ni by weight (*3*). Near the inner core boundary, the latent heat released by freezing out of the heavier metallic constituents and lighter Fe compounds with S, Si, or O has been suggested as the energy source that drives the geodynamo that generates the Earth's magnetic field (*4*). The extra buoyancy of the lighter compounds results in a stirring of the outer core by "compositional convection" (*5*), providing the necessary velocity field for the geomagnetic dynamo.

A layer about 450 km thick surrounding the inner core, called the F-layer, is part of the earliest Earth models derived from seismic wave observations (*6*). It was based on seismic waves interpreted as having been scattered by a possibly semisolid layer outside the inner core. More recent, improved observations have shown that the scattering could occur at the core-mantle boundary, but the two are not mutually exclusive (*7*). Stevenson (*8*) has argued, on the basis of liquid-state physics, that this region may differ in composition from the rest of the outer core. Jeanloz (*3*) estimates that as much as 50% by volume may consist of crystals mixed in the liquid alloy for an Fe-S composition compatible with the seismologically determined density. Here I consider a method of estimating the viscosity in the F-layer.

The solid inner core is suspended near the center of the outer fluid core by gravitational forces. The possibility of gravimetric observation of its bodily oscillations about its equilibrium position within the outer fluid core was discussed by Slichter (*9*), and the inner core's essentially rigid translational motions are often referred to as Slichter modes. There are three distinct modes, one along the axis of rotation, one prograde in the equatorial plane, and one retrograde in the equatorial plane. The axial mode period is reduced by about 0.6% by Earth's rotation, but the Coriolis acceleration acts to weaken the restoring force of the prograde equatorial mode, lengthening its period by about 7.8%, and acts to strengthen the restoring force of the retrograde equatorial mode, shortening its period by about 7.8%. Laws governing this splitting of the periods can be obtained directly from the equation of motion for the inner core. The splitting of the periods according to these laws can be used as a diagnostic tool and led to the association of three resonances in the frequency spectra obtained from superconducting gravimeter observations in Europe with the Slichter modes (*10*). An automated computer-based search across 4119 discrete periods suggests that no other triplet of resonances are correctly split (*11*). A recent analysis (*12*) of nearly 300,000 hours of superconducting gravimeter observations made at stations in Canada, China, Europe, Japan, and the United States has confirmed the presence of these spectral resonances with central periods, in what are considered to be best estimates, at 3.5822 ± 0.0012, 3.7656 ± 0.0015, and 4.0150 ± 0.0010 hours.

In the original identification (*10*), the theoretical periods were calculated assuming no viscosity in the outer core and on the basis of the subseismic or anelastic approximation (*13*) that applies when the fluid velocities are small compared with seismic velocities. The anelastic approximation neglects the inertia of the solid inner core and shell (*14*), but these are accounted for by the introduction of frequency-dependent internal load Love numbers (Love numbers, named for A. E. H. Love, are a compact way of expressing Earth's response to perturbing forces). A detailed discussion of the effects of the frequency dependence of Love numbers and several other controversial theoretical issues was presented earlier (*15*). Calculated inviscid periods for the two equatorial modes are then found to have a larger splitting than the observed periods. I show that the oversplitting can be used to estimate the effective viscosity near the inner core (boundary layer thickness, 370 km).

The translational modes of the inner core

Department of Earth and Atmospheric Science, York University, Toronto, Ontario M3J 1P3, Canada.

in the presence of viscosity can be regarded as an Ekman boundary layer problem (local and Coriolis acceleration balancing viscous forces in the boundary layer) for a sphere oscillating in a contained, rotating, and viscous fluid. This problem was solved (*16*), and explicit formulae for the drag forces exerted by the outer core fluid on the inner core were obtained for the three translational modes. These are expressed in terms of the corresponding pressure drag forces. For the axial mode, the viscous drag force is

$$D_v^a = \frac{1-i}{4}\sqrt{E_\mathrm{k}}\left(D_p^a + 4\Omega^2 M_\mathrm{I}'\sigma^2 U_\mathrm{I}\right)f^a(\sigma) \quad (1)$$

where

$$E_\mathrm{k} = \frac{\eta}{\Omega a^2 \rho_0}$$

is the dimensionless Ekman number. The dynamic viscosity is denoted by η, the angular rotation rate of Earth by Ω, the radius of the inner core by a, and the density outside the inner core by ρ_0. D_p^a is the pressure drag, M_I' is the mass the inner core would have if its actual density distribution were replaced by a uniform density ρ_0, σ is the angular frequency of the oscillation measured in units of twice the diurnal angular frequency of rotation 2Ω, and U_I is the amplitude of the motion. The viscous drag factor $f^a(\sigma)$ is a function of the dimensionless angular frequency σ given by

$$f^a(\sigma) = 8[(\sigma+1)^{3/2} + (\sigma-1)^{3/2}] - \frac{16}{5}[(\sigma+1)^{5/2} - (\sigma-1)^{5/2}] \quad (2)$$

For the two equatorial modes, the viscous drags, expressed in terms of the pressure drags D_p^e, are

$$D_v^e = \frac{1 \mp i}{8}\sqrt{E_k}\left(D_p^e + 4\Omega^2 M_I'\sigma(\sigma-1)U_\mathrm{I}\right)f^e(\sigma) \quad (3)$$

where the viscous drag factor $f^e(\sigma)$ is the function

$$f^e(\sigma) = \mp 24(\pm\sigma \mp 1)^{1/2} - 16(\pm\sigma \mp 1)^{3/2} - \frac{16}{5}[(\pm\sigma - 1)^{5/2} - (\pm\sigma + 1)^{5/2}] \quad (4)$$

plotted in Fig. 1. In Eqs. 3 and 4 the upper sign refers to the retrograde mode and the lower sign to the prograde mode. The dimensionless angular frequency σ is positive for the retrograde mode and negative for the prograde mode. In all cases, complex notation is adopted to keep track of phase, with the real part referring to in-phase components and the imaginary part denoting quadrature components.

The pressure drag forces D_p^a, D_p^e are approximated (*17*) by

$$4\Omega^2(\alpha\sigma^2 + \beta\sigma + \gamma)U_\mathrm{I} \quad (5)$$

where

$$\alpha = M_\mathrm{I}'\left(\frac{1}{2} + \frac{3}{2}\frac{M_\mathrm{I} + (a/b)^3 M_\mathrm{S}}{M_\mathrm{O} + M_\mathrm{S}(1-(a/b)^3)}\right)$$

for axial and equatorial modes, $\beta = 0$ for the axial mode and has the value

$$\beta = M_\mathrm{I}'\left(\frac{1}{4} - \frac{3}{4}\frac{M_\mathrm{I} + (a/b)^3 M_\mathrm{S}}{M_\mathrm{O} + M_\mathrm{S}(1-(a/b)^3)}\right)$$

for the two equatorial modes. In these expressions, the actual masses of the inner core, outer core, and shell are denoted by M_I, M_O, and M_S, respectively, while b is the radius of the outer core. The first term in the expression for α corresponds to the classic result that a sphere oscillating in an unbounded, inviscid fluid has an inertia augmented by half the displaced mass (*18*). The remaining term in the expression for α arises because the fluid is contained and linear momentum is conserved among the inner core, outer core, and shell. The term $\beta\sigma$ in Eq. 5—linear in frequency, arising in the case of equatorial, circular translational oscillations of a sphere in an inviscid, rotating fluid—is new. The term γ in Eq. 5, independent of frequency,

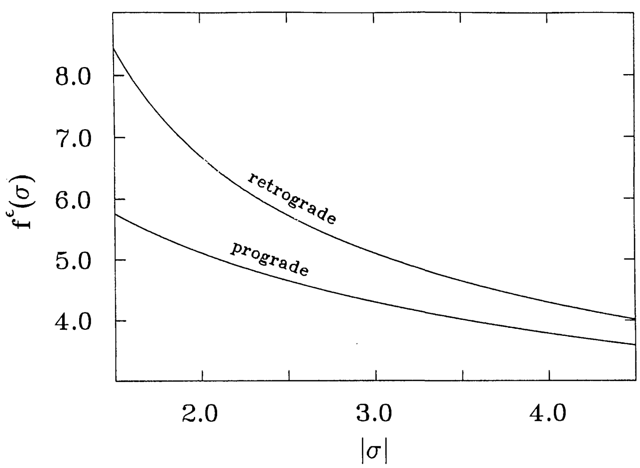

Fig. 1. Viscous drag factor $f^e(\sigma)$ as a function of the magnitude $|\sigma|$ of the dimensionless angular frequency σ. σ is positive for the retrograde mode, and negative for the prograde mode. The asymmetry of the drag factor provides a redundancy check on measures of viscosity obtained from the two equatorial translational modes of the inner core.

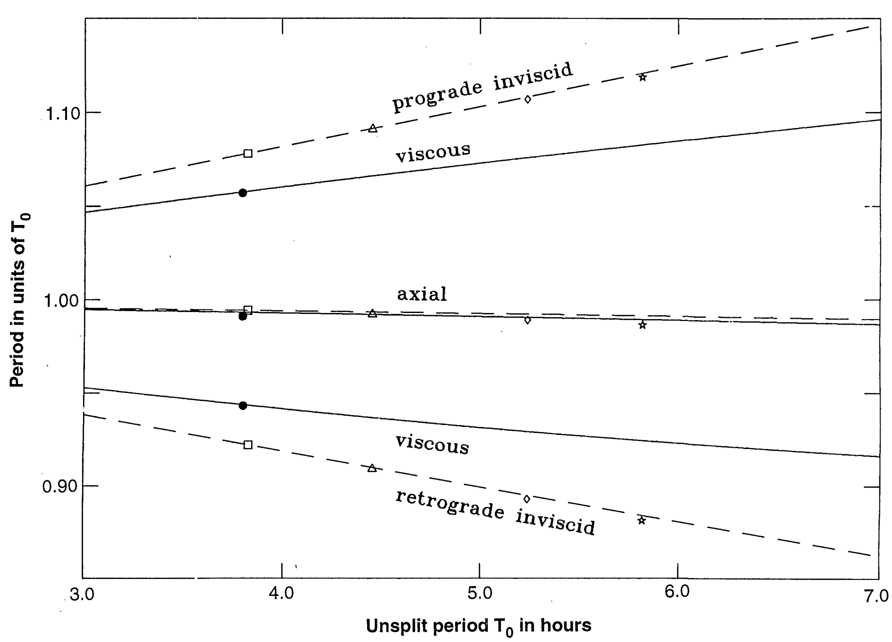

Fig. 2. Splitting curves for the three translational modes. The inviscid curves are shown dashed, based on the splitting parameters for Earth model Cal8 (*7*) (□). Inviscid periods are overplotted for Earth models 1066A (*21*) (△), PREM (*22*) (◇), and CORE11 (*23*) (☆). Solid curves represent viscous splitting for a single viscosity of 1.22×10^{11} Pa s. The splitting of the two equatorial modes is asymmetrically reduced, providing a strong redundancy check. The observed periods (●) are 6.12 s shorter than those predicted by the viscous splitting curves for the two equatorial modes.

does not arise in further discussions and I have omitted the rather complicated expression for it.

The equation of motion for the inner core leads directly to splitting laws of the form

$$\left(\frac{T}{T_0}\right)^2 + 2g\,\frac{T_0}{T_S}\left(\frac{T}{T_0}\right) - 1 = 0 \quad (6)$$

T is the period of the motion, T_S is the length of the sidereal day, T_0 is the unsplit period, and g is a dimensionless splitting parameter. For a given mode, g is nearly independent of Earth model (*19*). Inviscid periods and splitting parameters are computed by the variational method (*20*). With a viscous boundary layer around the inner core, the real part of the equation of motion yields a splitting law with viscous splitting parameter g^v related to the inviscid splitting parameter g^i for the axial mode by

$$g^v = g^i\left[1 + \frac{1}{4}\,\frac{M_I - M_I'}{M_I + \alpha}\,\sqrt{E_k}\,f^{\alpha}(\sigma)\right] \quad (7)$$

and by

$$g^v = g^i\left[1 - \frac{1}{8}\left(\frac{M_I' - \beta}{M_I + \beta} + \frac{M_I' + \alpha}{M_I + \alpha}\right)\sqrt{E_k}\,f^e(\sigma)\right] \quad (8)$$

for the equatorial modes.

The splitting parameter for the axial mode is small and the mode period is only reduced by about 0.1% by viscosity compared with its inviscid value. In contrast, the splitting parameters for the two equatorial modes are large and the periods are significantly modified by viscosity (the retrograde period is increased by 2.27% and the prograde period is decreased by 1.86% compared with their inviscid values). Furthermore, there is a built-in redundancy in using the viscous reduction of the rotational splitting of the two equatorial modes as measures of viscosity, in that the viscous drag factor $f^e(\sigma)$ given by Eq. 4 and illustrated in Fig. 1 is asymmetric for the two modes and tests the consistency of the calculations, because a single viscosity must produce the observed reduction in splitting for both equatorial modes. I find that this redundancy check is met to better than 0.04%. Splitting curves, based on Eq. 6, are plotted in Fig. 2 for all three modes with parameters for Earth model Cal8 of Bolt and Uhrhammer [see Appendix of (*7*)]. The inviscid splitting curves pass through the calculated inviscid periods for Cal8 and pass close to the calculated inviscid periods for Earth models 1066A (*21*), PREM (*22*), and CORE11 (*23*). Viscous splitting curves for the single recovered viscosity 1.225×10^{11} Pa s give periods 6.12 s longer than those observed for the retrograde and prograde equatorial translational modes.

Although the Ekman layer model gives an estimate of viscosity, it is not a unique model. Other possible causes for the observed reduction in splitting of the two equatorial modes need to be considered. One candidate is electromagnetic drag (*24*). Its effect was estimated and dismissed as negligible by Smylie (*10*) on the basis of field line tension. A similar conclusion was reached by Buffett and Goertz (*25*). Small skin depth (the depth to which a magnetic field penetrates a moving electrical conductor), about 100 m at translational mode periods, limits electromagnetic effects. In an axial field, the equatorial modes may be an exception as they would continuously cut field lines in the same sense, making the skin depth anomalously large. The ratio of the Lorentz force to the Coriolis acceleration scales as $B^2\Sigma/2\Omega\rho_0$, where B is the field strength and Σ is the electrical conductivity. Substitution of typical values (*26*) indicates that the Lorentz force could be significant compared with the Coriolis acceleration, but by Lenz's law it can only oppose the motion causing the induction, and therefore is orthogonal to the Coriolis effect and cannot reduce rotational splitting.

Although the viscosity we obtained is similar in magnitude to the anomalous bulk viscosity found by Stevenson (*27*), and although similar diffusive processes of heat and matter must arise from shear stress fluctuations, no parallel theory exists for the shear viscosity appropriate to the Ekman layer. Short-period seismic waves reflect sharply off the inner core boundary (*7*), but at longer periods the upper layers of the inner core may exhibit some shear relaxation, and my estimated viscosity might reflect this effect (*28*).

References and Notes

1. J. A. Jacobs, *Nature* **172**, 297 (1953).
2. F. D. Stacey, *Physics of the Earth* (Brookfield Press, Brisbane, Australia, ed. 3, 1992), p. 283.
3. R. Jeanloz, *Annu. Rev. Earth Planet. Sci.* **18**, 357 (1990).
4. S. I. Braginsky, *Dokl. Akad. Nauk SSSR* **149**, 8 (1963).
5. D. E. Loper and P. H. Roberts, *Phys. Earth Planet. Int.* **24**, 302 (1981).
6. K. E. Bullen, *An Introduction to The Theory of Seismology* (Cambridge Univ. Press, New York, ed. 3, 1965), pp. 220–242.
7. K. E. Bullen and B. A. Bolt, *ibid.* (Cambridge Univ. Press, New York, ed. 4, 1985), pp. 321–324 and Appendix. The Earth model Cal8 of Bolt and Uhrhammer given in the Appendix has low *P*-velocity gradient in the lower 450 km of the outer core and a relatively large density jump at the inner core boundary (1170 kg/m^3). The viscous translational mode periods for this Earth model are in close agreement with those observed.
8. D. J. Stevenson, *Phys. Earth Planet. Int.* **22**, 42 (1980).
9. L. B. Slichter, *Proc. Natl. Acad. Sci. U.S.A.* **47**, 186 (1961).
10. D. E. Smylie, *Science* **255**, 1678 (1992).
11. ———, J. Hinderer, B. Richter, B. Ducarme, *Phys. Earth Planet. Int.* **80**, 135 (1993).
12. N. Courtier *et al.*, paper presented at the 6th Symposium of Study of the Earth's Deep Interior, Tours, France, 5 to 10 July 1998. A full journal paper has been accepted pending revisions for the Proceedings to be published in *Phys. Earth Planet. Int.*
13. G. A. Glatzmaier and P. H. Roberts, *Physica D* **97**, 81 (1996). In a self-gravitating, compressible fluid such as the outer core, the requirement is that F_RC is small where F_R is the Froude-to-Rossby number ratio Ω^2L/g_0 and C is the compressibility number $\rho_0 g_0 L/\lambda$ with g_0, ρ_0, λ, and L indicating characteristic values of gravity, density, adiabatic bulk modulus, and length, respectively (*29, 30*). For large-scale core oscillations F_RC amounts to no more than a few parts in 10^3.
14. The shell consists of the rocky mantle and crust surrounding the outer fluid core and extending from the core-mantle boundary of radius 3485 km to the surface.
15. D. E. Smylie and X. Jiang, *J. Geomag. Geoelectr.* **45**, 1347 (1993). The inner core's motion is close to that of a rigid body. The frequency dependence of the Shell Love numbers, although included, has a minor effect on the translational periods.
16. D. E. Smylie and D. G. McMillan, *Phys. Earth Planet. Int.* **106**, 1 (1998).
17. ———, paper presented at the 6th Symposium of the Study of the Earth's Deep Interior, Tours, France, 5 to 10 July 1998. A full journal paper has been submitted for the Proceedings to be published in *Phys. Earth Planet. Int.* Equation 5 derives from asymptotic solution of three simultaneous equations representing conditions at the two boundaries of the outer core, and the conservation of linear momentum between the inner core, outer core, and shell.
18. H. Lamb, *Hydrodynamics* (Dover, New York, ed. 6, 1932), p. 644.
19. The values of g for the retrograde equatorial, axial, and prograde equatorial modes for the four Earth models I use are as follows: Cal8 (0.50871, 0.03577, 0.47041); 1066A (0.51372, 0.04212, 0.46877); PREM (0.51841, 0.04996, 0.46545); and CORE11 (0.52176, 0.05590, 0.46283).
20. D. E. Smylie, X. Jiang, B. J. Brennan, K. Sato, *Geophys. J. Int.* **108**, 465 (1992). Finite elements, adapted to the symmetry of the solutions, are used in the outer fluid core to avoid the serious errors caused by Coriolis coupling when conventional vector spherical harmonics are used.
21. F. Gilbert and A. Dziewonski, *Philos. Trans. R. Soc. London Ser. A* **278**, 187 (1975).
22. A. Dziewonski and D. Anderson, *Phys. Earth Planet. Int.* **25**, 297 (1981).
23. R. Widmer, G. Masters, F. Gilbert, paper presented at the 17th International Conference on Mathematical Geophysics, Blanes, Spain, 20 to 25 June 1988.
24. Electromagnetic drag is the resistance to motion of an electrical conductor (the inner core) through a magnetic field (the strong geomagnetic field in the outer core).
25. B. A. Buffett and D. E. Goertz, *Geophys. J. Int.* **120**, 103 (1995).
26. For the typical values $B = 0.005$ T, $\Sigma = 3 \times 10^5$ S m^{-1}, $\Omega = 7.29 \times 10^{-5}$ rad s^{-1}, and $\rho_0 = 1.2 \times 10^4$ kg m^{-3}, the ratio is 4.3 for this exceptional case. In general, it is further reduced by the ratio of the skin depth (107 m) to the typical length scale of the magnetic field (10^6 m), and the effect of electromagnetic drag is negligible.
27. D. J. Stevenson, *J. Geophys. Res.* **88**, 2445 (1983). Stevenson considered the irreversible entropy production arising from the transient diffusive processes of heat and matter near inclusions for the first time. He showed that at the low frequencies (10^{-4} Hz) involved here, the bulk viscosity can have an upper limit as high as 10^{13} Pa s.
28. B. A. Buffet, *Nature* **388**, 571 (1997). Inner core viscosity is estimated from the limit imposed on relative inner core rotation by gravitational coupling of the inner core to density anomalies in the shell. Viscosity of the "solid" inner core is constrained to between 10^{16} and 10^{20} Pa s.
29. D. E. Smylie and M. G. Rochester, *Phys. Earth Planet. Int.* **24**,308 (1981).
30. D. E. Smylie, A. M. K. Szeto, M. G. Rochester, *Rep. Prog. Phys.* **47**, 855 (1984).

11 November 1998; accepted 12 March 1999